Measurement of the formation rate and the radiative decay of the muonic molecules $(p\mu^3\mathrm{He})^*$ and $(p\mu^4\mathrm{He})^*$

S. Tresch, F. Mulhauser, C. Piller, L. A. Schaller, L. Schellenberg, H. Schneuwly, Y.-A. Thalmann, and A. Werthmüller
Institut de Physique de l'Université, Pérolles, CH-1700 Fribourg, Switzerland

P. Ackerbauer, W. H. Breunlich, M. Cargnelli, B. Gartner, R. King, B. Lauss, J. Marton, W. Prymas, and J. Zmeskal
Institute for Medium Energy Physics, Austrian Academy of Sciences, A-1090 Wien, Austria

C. Petitjean
Paul Scherrer Institute, CH-5232 Villigen, Switzerland

M. Augsburger,* D. Chatellard,* J.-P. Egger, and E. Jeannet
Institut de Physique de l'Université, CH-2000 Neuchâtel, Switzerland

T. von Egidy, F. J. Hartmann, M. Mühlbauer, and W. Schott
Physik Department, Technische Universität München, D-85747 Garching, Germany

(Received 20 April 1998)

Formation and decay of the $(p\mu^3\mathrm{He})^*$ and $(p\mu^4\mathrm{He})^*$ molecules have been studied in binary-gas mixtures of $H_2+{}^3\mathrm{He}$ and $H_2+{}^4\mathrm{He}$ at 30 K. The muon ground-state transfer rates from hydrogen to the two helium isotopes were extracted from the time distribution of the 7-keV decay x rays of the muonic hydrogen-helium molecules, measured with a Ge detector. The obtained transfer rates are $\lambda_{p^3\mathrm{He}}=(0.46\pm0.15)\times10^8\ \mathrm{s}^{-1}$ and $\lambda_{p^4\mathrm{He}}=(0.42\pm0.07)\times10^8\ \mathrm{s}^{-1}$. The radiative branching ratios of the decay of the $(p\mu^3\mathrm{He})^*$ and $(p\mu^4\mathrm{He})^*$ molecules were determined by comparing the yields of the Lyman series of muonic hydrogen with the one of the 7-keV line with charge-coupled-device detectors. The ratios are in agreement with theoretical predictions. Muon transfer from excited states of muonic hydrogen to both helium isotopes was also observed. [S1050-2947(98)07010-3]

PACS number(s): 36.10.Dr, 34.70.+e, 82.30.Fi

I. INTRODUCTION

The muon transfer from hydrogen isotopes to helium isotopes acts as a scavenger in the muon-catalyzed fusion cycle, reducing the fusion yield, since helium is produced in both nuclear reactions and tritium decay. In contrast to the transfer mechanism from muonic hydrogen to heavier elements, the muonic charge exchange to helium proceeds mainly via the formation of a metastable muonic hydrogen-helium molecule [1,2]

$$(\mu x)_{1s}+\mathrm{He}\rightarrow[(x\mu\mathrm{He})^*e^-]^+ + e^-, \qquad (1.1)$$

where x is either a proton (p), a deuteron (d), or a triton (t). This short living molecule ($\sim10^{-12}$ s) is formed in the excited state $2p\sigma$, and decays to its unbound ground state $1s\sigma$ either by particle decay (dissociation), by Auger emission, or by the emission of a 7-keV x ray. The end products are a hydrogen nucleus and a muonic helium atom in the ground state. Therefore the detection of the characteristic x rays at 7 keV is a direct evidence of the formation and decay of such molecules.

The direct transfer rate $\lambda_{p\mathrm{He}}^{\mathrm{dir}}$ to the ground state,

$$(\mu p)_{1s}+\mathrm{He}\rightarrow p+(\mu\mathrm{He})_{1s}, \qquad (1.2)$$

was calculated by Matveenko and Ponomarev [3]. This rate is about one order of magnitude smaller than the transfer via molecular formation $\lambda_{p\mu\mathrm{He}}$ [Eq. (1.1)]. The total muon transfer rate from the ground state of muonic hydrogen to helium $\lambda_{p\mathrm{He}}$ is defined as the sum of the rates $\lambda_{p\mu\mathrm{He}}$ [Eq. (1.1)] and $\lambda_{p\mathrm{He}}^{\mathrm{dir}}$ [Eq. (1.2)].

This total muon transfer rate from hydrogen to ^{4}He has been measured in several experiments [4–8], and recently the transfer rate to ^{3}He was determined by the present collaboration [8]. Although different methods were used, the transfer rates have not been determined directly from the time distribution of the 7-keV line up to this experiment. In the lifetime measurements [4–6,8] a third gas was used as an indicator, and in the yield measurement [7] one had to rely on the calculated radiative branching ratio of the molecule.

In the present measurements, the total muon transfer rate from the ground state of hydrogen to ^{3}He and ^{4}He was determined by measuring the time distributions of the 7-keV x rays with a germanium detector in binary-gas mixtures $H_2+{}^3\mathrm{He}$ and $H_2+{}^4\mathrm{He}$ at 30 K. Using our transfer rates, the radiative branching ratio of the molecules was determined by measuring the yields of the Lyman series of muonic hydrogen at ~2 keV, and of the 7-keV molecular decay x rays using CCD (charged coupled device) detectors [9]. In addition, several characteristics of the transfer from excited states

*Present address: Institut de Physique de l'Université, Pérolles, CH-1700 Fribourg, Switzerland.

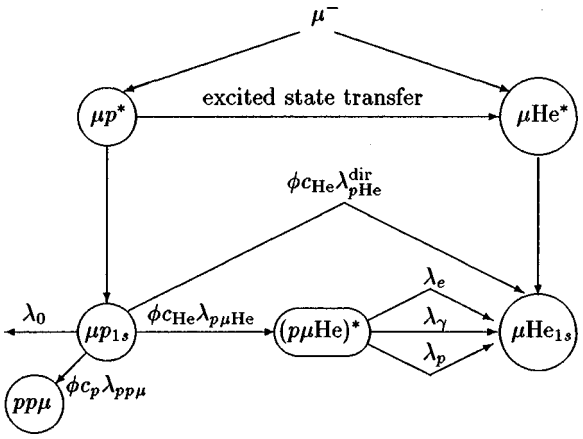

FIG. 1. Scheme of the main processes induced by a μ^- in a binary-gas mixture H_2+He. The starting processes are the formation of a muonic hydrogen atom $(\mu p)^*$ or a muonic helium atom $(\mu\mathrm{He})^*$ in an excited state. See text for an explanation of the symbols.

could be deduced from the measurements in the binary mixtures.

II. EXPERIMENTAL METHOD

The main processes of the muon in a binary mixture of H_2+He are presented in Fig. 1. A negative muon entering the gas target will be captured either by hydrogen or helium. The excited $(\mu p)^*$ or $(\mu\mathrm{He})^*$ atoms deexcite to their respective ground state $(\mu p)_{1s}$ and $(\mu\mathrm{He})_{1s}$. The muon transfer from an excited state of the muonic hydrogen $(\mu p)^*$ to an excited state of the muonic helium competes with the deexcitation of the $(\mu p)^*$ atom. From the ground state $(\mu p)_{1s}$, the muon disappears either by decay with a rate $\lambda_0=4.5516\times10^5\ \mathrm{s}^{-1}$ [10], by formation of a $pp\mu$ molecule with a rate $\lambda_{pp\mu}=(2.34\pm0.17)\times10^6\ \mathrm{s}^{-1}$ [11], by transfer to helium ($\lambda_{p\mathrm{He}}$) or by transfer to impurities such as deuterium with a rate $\lambda_{pd}=(1.43\pm0.13)\times10^{10}\ \mathrm{s}^{-1}$ [12]. The transfer and formation rates are all normalized to the atomic liquid hydrogen density (LHD, 4.25×10^{22} atoms cm^{-3}). As already mentioned (see also Fig. 1), the muon transfer from the $(\mu p)_{1s}$ ground state to helium proceeds either by an intermediate molecule or by direct transfer. The latter is suppressed by one order of magnitude [3]. In this experiment the total transfer rate $\lambda_{p\mathrm{He}}$ is measured, which is the sum of the direct transfer rate $\lambda_{p\mathrm{He}}^{\mathrm{dir}}$ and the molecular formation rate $\lambda_{p\mu\mathrm{He}}$. The observed disappearance rate $\Lambda_{\mu p_{1s}}$ of the $(\mu p)_{1s}$ level is equivalent to the sum of the rates of the various disappearance channels:

$$\Lambda_{\mu p_{1s}}=\frac{1}{\tau_{\mu p_{1s}}}=\lambda_0+\phi(c_p\lambda_{pp\mu}+c_d\lambda_{pd}+c_{\mathrm{He}}\lambda_{p\mathrm{He}}). \tag{2.1}$$

Here $\tau_{\mu p_{1s}}$ is the measured lifetime of the $(\mu p)_{1s}$ atom, ϕ is the atomic gas density relative to the LHD, and c_j is the atomic concentration of the element j.

Contrary to the triple-gas mixture method [8], where the disappearance rate is determined from the time distributions of the muonic x rays from the added third gas component, in binary mixtures $\Lambda_{\mu p_{1s}}$ is obtained from the time distribution of the 7-keV molecular decay x rays. Therefore, the total muon transfer rate from hydrogen to helium $\lambda_{p\mathrm{He}}$ can be calculated using Eq. (2.1).

The radiative branching ratio κ of the $(p\mu\mathrm{He})^*$ molecules is given by

$$\kappa=\frac{\lambda_\gamma}{\lambda_p+\lambda_e+\lambda_\gamma}, \tag{2.2}$$

where λ_p, λ_e, and λ_γ are the decay rates of the molecule due to particle decay, Auger transition, and radiative decay, respectively. The ratio κ can be extracted from the relation

$$\frac{N_{7\text{-keV}}}{N_{\mu p}}=\kappa W, \tag{2.3}$$

where $N_{7\text{-keV}}$ is the yield of the 7-keV decay x rays, and $N_{\mu p}$ the yield of the Lyman series intensities from muonic hydrogen, i.e., the number of μp atoms reaching the ground state. W is the probability that a $(p\mu\mathrm{He})^*$ molecule is formed from the ground state of the muonic hydrogen atom. It is expressed by

$$W=\frac{\phi c_{\mathrm{He}}\lambda_{p\mu\mathrm{He}}}{\lambda_0+\phi(c_p\lambda_{pp\mu}+c_d\lambda_{pd}+c_{\mathrm{He}}\lambda_{p\mathrm{He}})}=\frac{\phi c_{\mathrm{He}}\lambda_{p\mu\mathrm{He}}}{\Lambda_{\mu p_{1s}}}. \tag{2.4}$$

The yields of $N_{7\ \mathrm{keV}}$ and $N_{\mu p}$ are measured with CCD detectors. A contribution to the yield of $N_{7\ \mathrm{keV}}$ from excited-state transfer can be neglected, since this transfer occurs predominantly by direct charge exchange and not via molecular formation [13].

It should be mentioned that a small deuterium contamination strongly contributes to the yield of the radiative decay x rays of the $(p\mu\mathrm{He})^*$ molecules. This is due to the high transfer rate to deuterium (λ_{pd}), the high molecular formation rate $\lambda_{d\mu\mathrm{He}}$ (about 5–25 times $\lambda_{p\mu\mathrm{He}}$ [14], depending on the helium isotope), and the high radiative branching ratio κ in the decay of the $(d\mu\mathrm{He})^*$ molecules [about 30–50 % compared to only 3–7 % of the $(p\mu\mathrm{He})^*$ molecules [15]]. Therefore, the use of pure hydrogen gas is extremely important.

III. TARGET AND DETECTION SYSTEM

The experiment was performed at the $\mu E4$ channel of the Paul Scherrer Institute (PSI) in two run periods, a first one for the mixture $H_2+{}^4\mathrm{He}$ and a second for the mixture $H_2+{}^3\mathrm{He}$ (see Table I). The hydrogen gas was produced by electrolysis of deuterium depleted water, where a deuterium contamination of less than 2 ppm is guaranteed. The online analysis of the gas mixture with a high-resolution mass spectrometer revealed no impurities. For a possible deuterium contamination due to the filling system, a conservative upper limit of 20 ppm has been estimated.

The primary proton beam current was 1.0 mA in the first run and 1.5 mA in the second run. Negative muons with a momentum of 35.6 MeV/c were focused on the target center as a 2.0×1.5 cm^2 beam spot. Under these conditions, typi-

TABLE I. Characteristics of the gas mixtures H_2+He and of the pure helium targets.

Gas	Atomic gas concentration c_H (%)	Atomic gas concentration c_{He} (%)	Density ϕ (% of LHD)	Pressure (bar)	Temperature (K)
$H_2+{}^3He$	88.2±0.3	11.8±0.3 (^{3}He)	5.20±0.05	3.72±0.01	26.2±0.1
$H_2+{}^4He$	86.80±0.04	13.20±0.04 (^{4}He)	7.36±0.08	5.15±0.01	26.5±0.2
^4He		100 (^{4}He)	3.95±0.03	4.71±0.01	20.5±0.2
^3He		100 (^{3}He)	2.60±0.02	3.19±0.01	21.0±0.1

cally 26 000 muons/s entered the target. In each run period, the target cell was filled with pure hydrogen and pure helium gas to observe the cascade x rays undisturbed from transfer processes.

Target apparatus and gas handling system were used in our previous experiment [8], and more details can be found in Refs. [16–18]. The detector arrangement for the present experiment is shown schematically in Fig. 2. The target cell was made from aluminum and was coated by a thin silver layer in the $H_2+{}^3He$ run. The target cell windows could withstand pressures up to 6 bar. Hence a high muon stopping rate was achieved at low temperatures around 30 K. X-ray detectors were placed on both sides of the target cell: a CCD detection system on one side and a germanium detector on the other side. The target windows were a 23-μm Hostaphan foil on the CCD side and a 50-μm Kapton foil on the germanium detector side. The CCD's were kept in vacuum, separated from the target by a 12-μm Mylar window.

Four plastic scintillators of 0.5-cm thickness were placed around the target vessel. These scintillators were used as muon decay electron counters. The background for the muonic x-ray spectra could be strongly reduced by requiring for each x-ray event a delayed electron from the muon decay within 0.2–4.0 μs relative to the muon stop (delayed-electron condition).

The time and energy information for the determination of the muon ground-state transfer rate was obtained from the germanium detector. In the $H_2+{}^4He$ run, a 0.25-cm^3 detector was placed at a distance of 8 cm from the target center. Its useful energy range started at 5 keV and extended up to 70 keV. In the $H_2+{}^3He$ run, a 0.17-cm^3 detector was used, with a useful energy range from 3 to 30 keV. For the μHe(2–1) transition at 8.2 keV in pure helium, the time resolution was 25 ns (30 ns) and the energy resolution 250 eV (170 eV) for the 0.25-cm^3 (0.17-cm^3) Ge detector.

Radiative transitions in the energy range between 1.5 and 11 keV were detected by two CCD detectors. CCD's as soft-x-ray detectors have been described in detail, e.g., in Refs. [9,19]. Each CCD chip had a size of 4.5 cm^2 (770×1152 pixels of area 22.5×22.5 μm^2). The depletion depth was ~30 μm [20]. The useful energy range was between ~1.5 (limited by the thickness of the pixel electrodes) and 12 keV (limited by the depletion depth). An energy resolution of 120 eV [full width at half maximum (FWHM)] was obtained in the measurement of the μH(2–1) transition at 1.9 keV. The CCD's yielded no timing information. The data were read out approximately every 3 min by a data-acquisition system which operated independently from the data acquisition of the other detectors.

The excellent two-dimensional spatial resolution of the CCD's turns out to be decisive to extract a weak signal out of a large background. In most cases, x rays produce single-pixel events, whereas the track of charged particles produces events in a cluster of pixels. The usual way to distinguish soft-x-ray events from background is to require a hit in one single pixel with none of the eight surrounding pixels having a charge above the noise level. The CCD analysis and background rejection are described in detail in Refs. [18,19,21].

The relative efficiency of the CCD detection system is determined by the transmission of the x rays through the

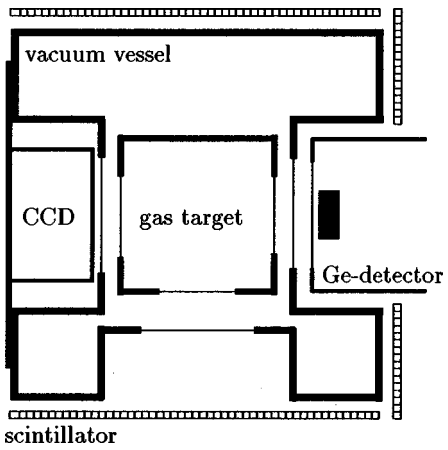

FIG. 2. Schematic target setup as viewed by the entering muons. The thin lines represent target and detector windows, as described in the text. The drawing is not to scale.

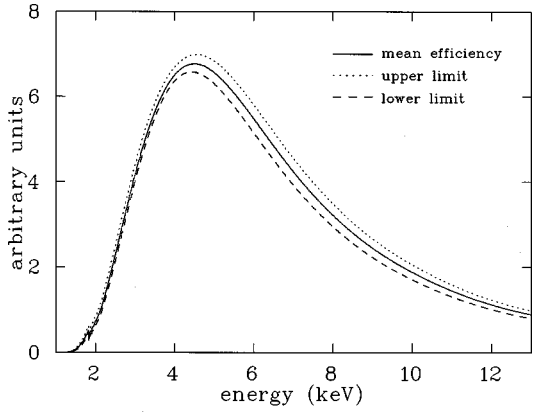

FIG. 3. Relative efficiency of the CCD detection system including absorption by the target windows. The small but sharp fall in the curve at 1.7 keV is due to the *K* edge of silicon, the main material of the CCD. The dashed lines represent the limits of the 1σ error band.

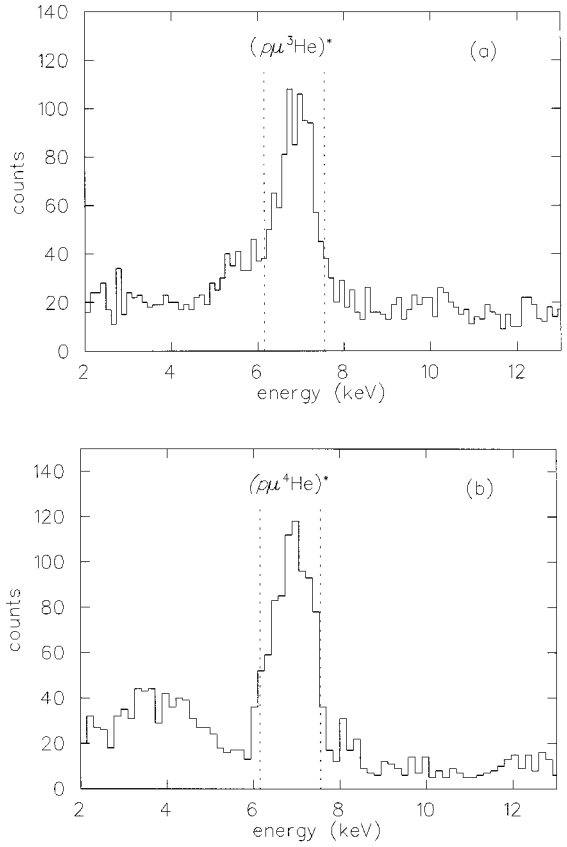

FIG. 4. Energy spectra of the decay x rays from the molecules $(p\mu^3\mathrm{He})^*$ and $(p\mu^4\mathrm{He})^*$ taken with Ge detectors. The given events are delayed with respect to stopping muons and in delayed coincidence with muon decay electrons. The dashed lines indicate the energy range of the events of which the time distributions were analyzed (cf. Fig. 5).

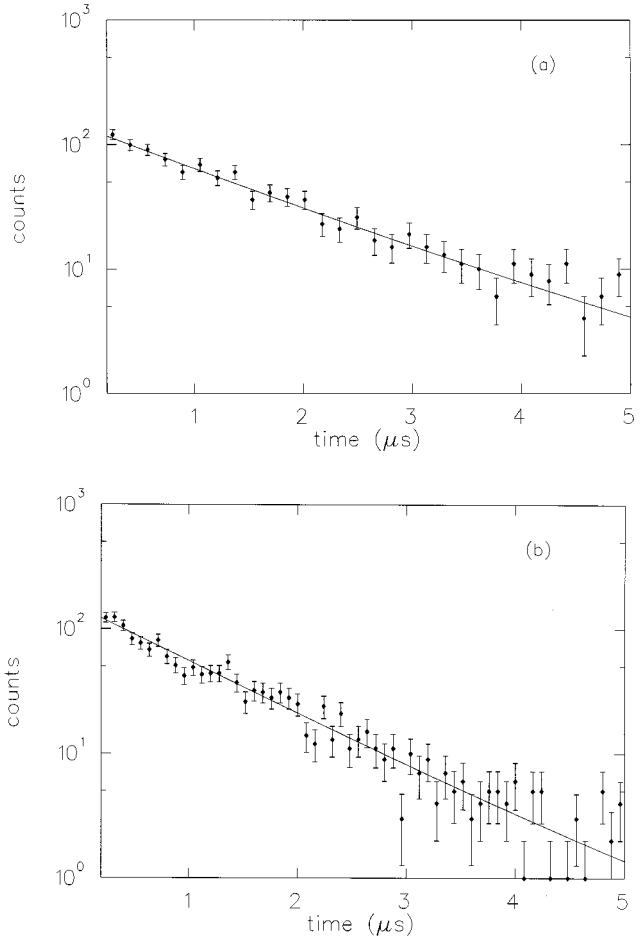

FIG. 5. Time distributions of the decay x rays from $(p\mu^3\mathrm{He})^*$ molecules (a) and from $(p\mu^4\mathrm{He})^*$ molecules (b). The full lines represent the fit to the data.

different foils, and the intrinsic efficiency of the CCD chips. The efficiency due to photoabsorption in the material was calculated using known absorption coefficients [22]. The chemical composition of the Mylar, Hostaphan and Kapton foils can be found in Refs. [23–25], and the CCD composition in Refs. [20,21]. The relative efficiency of the CCD detection system (CCD's with target windows) is shown in Fig. 3. Small corrections such as those for the deformation of the target windows (due to the target pressure) and the variation of thickness of the CCD absorption layers (due to the angular spread of incident x rays) [18] have been considered. The calculated uncertainties are 17% at 2 keV and 8% at 7 keV. Our intrinsic efficiency agrees with the one given in Ref. [19], and with the measured efficiency of Ref. [18] (measurements of antiprotonic gases at very low pressure and Kβ/Kα ratios of electronic x rays).

IV. RESULTS AND DISCUSSION

A. Muon transfer rates from $(\mu p)_{1s}$ to ^{3}He and ^{4}He

The 7-keV decay x rays from the molecules $(p\mu^3\mathrm{He})^*$ and $(p\mu^4\mathrm{He})^*$ have been measured with Ge detectors in binary hydrogen plus helium gas mixtures (see Table I). The energy spectra in Fig. 4 show the 7-keV molecular transitions of the $(p\mu^3\mathrm{He})^*$ and $(p\mu^4\mathrm{He})^*$ molecules, which show the formation of such molecules by muon transfer from hydrogen to ^{3}He and to ^{4}He, respectively. These spectra contain only events which are delayed with respect to the muon stop in the target, and followed by a muon decay electron. Under these conditions, electronic x rays from surrounding materials and the prompt muonic x rays from direct capture in helium are suppressed. The wide ''bump''around 4 keV in the $H_2+{}^4$He spectrum [Fig. 4(b)] is due to the increasing background and the decreasing sensitivity of the constant fraction module at the low-energy side. In the $H_2+{}^3$He run [see Fig. 4(a)], a smaller Ge detector was used, resulting in less background at low energies. The stronger asymmetry on the left side of the 7-keV line in $(p\mu^3\mathrm{He})^*$ is mainly due to background.

The positions of the maximum height of the 7-keV peaks are determined to be 7.00 ± 0.06 keV for the $(p\mu^3\mathrm{He})^*$ molecule and 7.05 ± 0.04 keV for $(p\mu^4\mathrm{He})^*$. A direct comparison of our measured spectrum [Fig. 4(b)] with predictions of energy and shape of the 7-keV line in the molecule $(p\mu^4\mathrm{He})^*$, was performed in Refs. [26,27]. These comparisons show good agreement for the energy, the asymmetry and the width of about 850 eV (FWHM).

The time distributions of the 7-keV x rays were obtained by using only events in the energy interval 6.1 keV$<E<$7.5 keV. These distributions are shown in Fig. 5. The time spectra were fitted by a sum of two exponential functions, one for the lifetime of the $(\mu p)_{1s}$ atom, and one to take into account

TABLE II. Experimental and theoretical muon transfer rates from hydrogen to ^{4}He at low ($\sim$30 K) and at room temperature.

Temperature (K)	Mixture	Experiment $\lambda_{p^4\mathrm{He}}$ (10^8 s^{-1})	Theory $\lambda_{p\mu^4\mathrm{He}}$ (10^8 s^{-1})	Reference
26	$H_2+{}^4$He	0.42 ± 0.07		this work
27.8	$H_2+{}^4$He+Ne	0.55 ± 0.07		[8]
27	average	0.49 ± 0.05 [a]		
30			0.47	[1]
30			0.43	[29]
30			0.46–0.64	[14]
300	$H_2+{}^4$He+Xe	0.36 ± 0.10		[4]
300	$H_2+{}^4$He+Ar	0.51 ± 0.19		[6]
300	$H_2+{}^4$He	0.44 ± 0.20 [b]		[7]
300	$H_2+{}^4$He+Ne	0.43 ± 0.04		[30]
300			0.32–0.52	[1,29,14]

[a]Average value of Ref. [8] and this experiment.

[b]This rate was corrected from the original work by taking into account the particle decay rate of Ref. [15].

the background. The spectra were fitted in the time interval $0.3\ \mu\mathrm{s}<T<3.0\ \mu\mathrm{s}$ after the prompt peak. The analysis yielded $(\mu p)_{1s}$ lifetimes of $\tau_{\mu p_{1s}}=1180\pm150$ ns in the $H_2+{}^3$He mixture and $\tau_{\mu p_{1s}}=990\pm61$ ns in the $H_2+{}^4$He mixture. Using Eq. (2.1), the total transfer rates from the ground state of muonic hydrogen to ^{3}He and ^{4}He were evaluated to be

$$\lambda_p^3\mathrm{He}=(0.46\pm0.15)\times10^8\ \mathrm{s}^{-1},$$

$$\lambda_p^4\mathrm{He}=(0.42\pm0.07)\times10^8\ \mathrm{s}^{-1}.$$

For both rates, the main contribution to the error is the uncertainty of the determined lifetime $\tau_{\mu p_{1s}}$. Other contributions, such as the uncertainty of the gas densities, the gas concentrations, and the other rates, are relatively small.

Our experimental results on the total muon transfer rates from hydrogen to the two helium isotopes, and the theoretical predictions of the molecular formation rates are presented in Tables II and III. The muon transfer rates obtained by our group from the triple-gas mixture method [8] are, within the error limits, in agreement with the present rates. Hence the weighted average muon transfer rate at 30 K from hydrogen to the two helium isotopes are $\langle\lambda_{p^3\mathrm{He}}\rangle=(0.36\pm0.08)\times10^8$ s^{-1} and $\langle\lambda_{p^4\mathrm{He}}\rangle=(0.49\pm0.05)\times10^8$ s^{-1}. These rates correspond to the sum of molecular formation and direct transfer. If direct transfer can be neglected [28], our total transfer rates would be molecular formation rates. If direct transfer cannot be neglected [3], we would obtain the molecule formation rates $\lambda_{p\mu^3\mathrm{He}}=(0.30\pm0.08)\times10^8$ s^{-1} and $\lambda_{p\mu^4\mathrm{He}}=(0.43\pm0.05)\times10^8$ s^{-1} by subtracting from our averaged total rates the direct transfer rates as calculated by Matveenko and Ponomarev [3].

In both cases, the obtained transfer rates at 30 K to ^{4}He agree well with the predicted rates in Refs. [1,14,29]. Together with a measurement at room temperature [30], they do not contradict the expected temperature dependences. In contrast to the good agreement in the ^{4}He case, the rates for ^{3}He ($\lambda_{p^3\mathrm{He}}$, $\lambda_{p\mu^3\mathrm{He}}$) are smaller by a factor of 2–3 than the corresponding theoretical predictions (cf. Table III). This discrepancy remains unexplained.

B. Radiative decay ratio κ of the molecules $(p\mu^3\mathrm{He})^*$ and $(p\mu^4\mathrm{He})^*$

The x-ray yields of the Lyman series of muonic hydrogen, muonic helium, and the 7-keV line were simultaneously observed with CCD detectors. The energy spectrum for the $H_2+{}^4$He gas mixture is shown in Fig. 6. The good energy

TABLE III. Experimental and theoretical muon transfer rates from hydrogen to ^{3}He at low temperature ($\sim$30 K).

Temperature (K)	Mixture	Experiment $\lambda_{p^3\mathrm{He}}$ (10^8 s^{-1})	Theory $\lambda_{p\mu^3\mathrm{He}}$ (10^8 s^{-1})	Reference
26	$H_2+{}^3$He	0.46 ± 0.15		this work
26	$H_2+{}^3$He+Ne	0.29 ± 0.12		[8]
26	average	0.36 ± 0.08 [a]		
30			0.91	[1]
30			0.64	[29]
30			0.81–1.10	[14]

[a]Average value of Ref. [8] and this experiment.

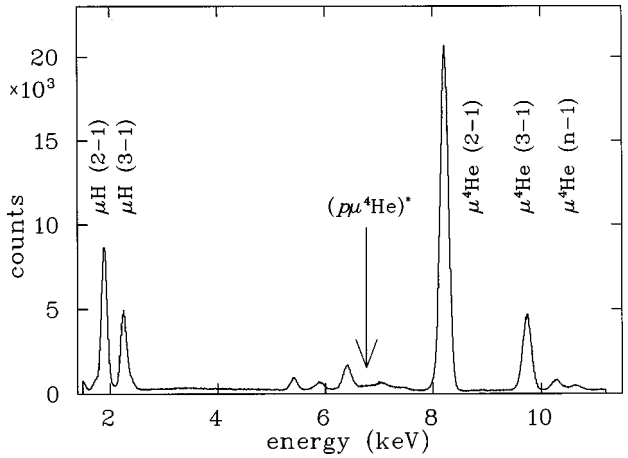

FIG. 6. Energy spectrum measured by the CCD detectors in the $H_2+{}^4He$ gas mixture. One observes the Lyman series of muonic hydrogen at ~2 keV, electronic x rays of Cr, Mn, Fe, Ni, and Cu in the region of the $(p\mu^4He)^*$ decay x rays, and the Lyman series of muonic helium.

resolution at 2 keV [the μH(2–1) and the μH(3–1) lines are clearly separated] and the excellent peak-to-background ratio should be noted. Compared to the muonic hydrogen and helium x rays, the yield of the 7-keV line is rather small (also see Fig. 7).

In the vicinity of the 7-keV line, the smooth accidental background was approximated by a polynomial function of second order. This background was subtracted. The resulting energy spectra are shown in Fig. 7. Since timing conditions, and in particular the delayed-electron condition, cannot be applied in the analysis of the CCD-detection system, the electronic x rays of Cr, Mn, Fe, and Ni could not be suppressed. In the $H_2+{}^3He$ run, the target was coated by a thin silver layer. This way the yield of the electronic x-ray lines could be reduced. As a result, the Cr $K\alpha$ peak almost disappeared, and much smaller Mn $K\alpha$ and Fe $K\alpha$ peaks are observed (see Fig. 7).

To fit the asymmetric 7-keV lines, we used the theoretical line shapes as given for the decay from the molecular state with total angular momentum $J=1$ [26], taking the efficiency of the CCD detection system into account. The electronic x-ray lines were fitted by Gaussian functions. The intensity ratios $K\alpha/K\beta$ and the corresponding energy differences were taken from Ref. [31]. The yields of the 7-keV decay x rays are $N_{7\text{-keV}}=18\,400\pm3\,000$ for the $(p\mu^3He)^*$ molecule and $N_{7\text{-keV}}=61\,800\pm6\,400$ for the $(p\mu^4He)^*$ molecule. The errors include the uncertainty of the detector efficiency, the statistical error as taken from the fit, and the uncertainty of the background subtraction.

The yields of the Lyman series of muonic hydrogen $N_{\mu p}$ were derived from fits with Gaussians. We obtained $N_{\mu p}=(1.1\pm0.2)\times10^6$ events in the $H_2+{}^3He$ mixture and $N_{\mu p}=(2.1\pm0.3)\times10^6$ events in the $H_2+{}^4He$ mixture. The errors are mainly due to the uncertainty in the efficiency. The contribution of the Balmer series of muonic helium in the region of the Lyman series of muonic hydrogen can be obtained in the pure He CCD spectra, and is less than 2%.

The radiative branching ratio κ is determined by using Eqs. (2.3) and (2.4). Under the assumption that one can neglect direct ground-state transfer to helium [28], the total

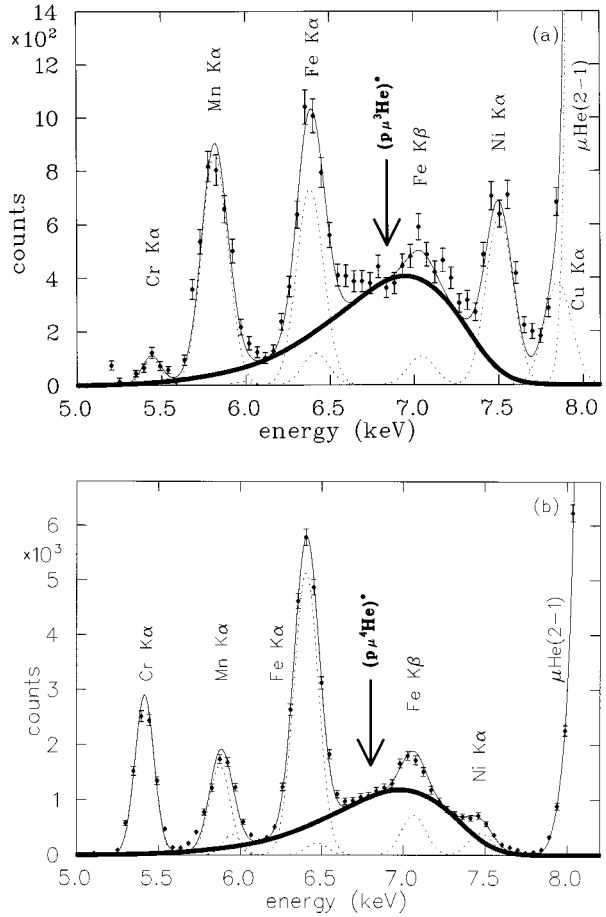

FIG. 7. Energy spectra of the CCD's with accidental background subtracted in the region of the decay x rays of the molecules $(p\mu^3He)^*$ and $(p\mu^4He)^*$. The decay x-ray peaks at 7 keV are shown as bold lines. The full line represents the fit to the data. The dashed lines are the contribution of the various electronic $K\alpha$ and $K\beta$ x rays.

transfer rates $\langle\lambda_{p^4He}\rangle=(0.49\pm0.05)\times10^8\ s^{-1}$ and $\langle\lambda_{p^3He}\rangle=(0.36\pm0.08)\times10^8\ s^{-1}$ become equal to the molecular formation rates. The resulting ratios κ are

$$p\mu^3He:\kappa=0.060\pm0.019,$$

$$p\mu^4He:\kappa=0.060\pm0.012.$$

If we take direct ground-state transfer to helium into account [3], the molecular formation rates change to $\lambda_{p\mu^4e}=(0.43\pm0.05)\times10^8\ s^{-1}$ and $\lambda_{p\mu^3He}=(0.30\pm0.08)\times10^8\ s^{-1}$. In this case, the branching ratios κ become

$$p\mu^3He:\kappa=0.070\pm0.023,$$

$$p\mu^4He:\kappa=0.068\pm0.014.$$

The uncertainties are root-mean-square (rms) errors of statistical and systematical uncertainty, such as background subtraction, the efficiency of the CCD's, the absorption by the target window, the gas density, the gas concentration, and the transfer and formation rates. As mentioned in Sec. II, a small deuterium contamination has a strong influence on the yield of the 7-keV line. With an estimated upper limit of

TABLE IV. Measured values and predictions for the radiative branching ratio κ of the decay of the $(p\mu^3\mathrm{He})^*$ and $(p\mu^4\mathrm{He})^*$ molecules.

	$(p\mu^3\mathrm{He})^*$	$(p\mu^4\mathrm{He})^*$
This work	$0.060\pm0.019^{a,b}$	$0.060\pm0.012^{a,b}$
This work	$0.070\pm0.023^{c,b}$	$0.068\pm0.014^{c,b}$
Theory [15]	0.051	0.069
Theory [26]	0.034	0.045
Theory [32]	0.034	0.048

[a]With the assumption that the direct transfer rate may be neglected [28].

[b]With an estimated upper limit of 20 ppm deuterium content in the target, an additional systematic error of $(^{+0.000}_{-0.020})$ has to be included.

[c]Determined using the calculated rates [3] for the direct muon transfer. $\lambda^{\mathrm{dir}}_{p^3\mathrm{He}}=0.063\times10^8\ \mathrm{s}^{-1}$ and $\lambda^{\mathrm{dir}}_{p^4\mathrm{He}}=0.055\times10^8\ \mathrm{s}^{-1}$.

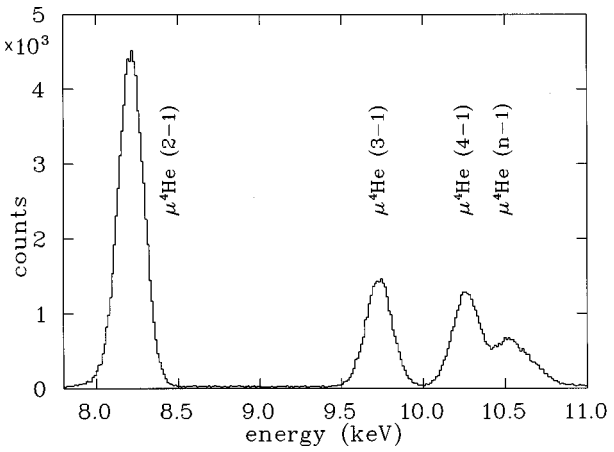

FIG. 8. Energy spectrum of the muonic Lyman x rays measured from pure ^{4}He as measured with CCD detectors.

20 ppm of deuterium, an additional systematical error of $^{+0.000}_{-0.020}$ has to be included in the above values.

The experimental branching ratios κ are compared with theory [15,26,32] in Table IV. Our results confirm the small radiative branching ratio for the $(p\mu\mathrm{He})^*$ molecules in comparison with the ones for the $(d\mu\mathrm{He})^*$ molecules.

C. Transfer from excited μp^* atoms to ^{3}He and ^{4}He

Theory predicts rates for muon transfer from the excited states of muonic hydrogen to helium of the order of $10^{11}-10^{12}\ \mathrm{s}^{-1}$ [13]. With such high rates, the muon transfer competes with the deexcitation process of the muonic hydrogen atom. The intensity pattern of the Lyman series of muonic helium in H_2+He mixtures (the sum of the ''direct cascade'' plus ''excited state transfer cascade'') is then expected to be different from the one in pure helium, where only direct muon capture occurs (direct cascade). We assume that the intensity ratios of the direct cascade in the gas mixture do not differ significantly from those measured in pure helium gas. Nonradiative transitions to the ground state are considered to be negligible. Measurements of the muonic Lyman series intensities in pure ^{3}He and ^{4}He were performed at gas densities comparable to those for the binary mixtures (Table I). The analysis of the muonic x-ray spectra taken with the CCD detectors yielded the same intensity pattern for both helium isotopes. The mean values for the transition intensities are given in Table V. Our result agrees well with the result of Ref. [33]. The energy difference $\Delta E(^4\mathrm{He}-{}^3\mathrm{He})=75.0\pm1.0$ eV of the $2p$-$1s$ transitions between the two helium isotopes corresponds to the expected energy shift [34].

Significant differences are observed between the intensity patterns of the Lyman series of muonic helium in pure ^{4}He gas (Fig. 8) and in the $H_2+{}^4$He mixture (Fig. 6). In the mixture, the μHe(2–1) and μHe(3–1) transitions are clearly favored and the higher transitions are strongly suppressed. This is further illustrated in Fig. 9, where the spectrum of muonic helium from pure ^{4}He (only direct muon capture) is subtracted from the spectrum taken in the binary mixture $H_2+{}^4$He. For this purpose, the spectrum of pure ^{4}He was normalized to the ^{4}He density in the mixture, and to the total muon stops by comparing the background in the 3–5 keV region. What remains are the events due to excited-state transfer. This leads to the conclusion that the muon transfer from the excited $(\mu p)^*$ states populates mainly levels with quantum numbers $n=2$ and $n=3$, as was also observed with a measurement performed at about ten times lower density [35]. The same holds true for the excited-state transfer to ^{3}He, as can be seen from Table V. The small dips in the region of the $\mu\mathrm{He}(n-1)$ transitions, $n>3$ (Fig. 9), points to the limits of the chosen subtraction procedure.

With the assumption that no levels with $n>3$ are populated by transfer, the intensity of the μHe(4–1) transition can be used as another normalization. Again the He spectrum is subtracted from the one obtained in H_2+He. The resulting energy spectrum is in good agreement with the one obtained by the first normalization. The intensities of the Lyman se-

TABLE V. Relative muonic x-ray intensities of the Lyman series in helium measured in pure He (^{3}He, ^{4}He) and in the mixtures $H_2+{}^3$He and $H_2+{}^4$He. The last two columns show the relative intensities resulting from excited-state transfer (cf. text). The sum of the Lyman series intensities is normalized to 100.

	Muonic x-ray intensities (%)			Excited-state transfer (%)	
Transition	He	$H_2+{}^3$He	$H_2+{}^4$He	^{3}He	^{4}He
μHe(2–1)	47.0 ± 0.2	64.0 ± 0.2	71.1 ± 0.2	67.9 ± 0.3	75.3 ± 0.3
μHe(3–1)	20.3 ± 0.1	27.6 ± 0.1	24.1 ± 0.1	32.1 ± 1.3	24.7 ± 1.3
μHe(4–1)	19.8 ± 0.1	5.3 ± 0.1	3.5 ± 0.1	0	0
μHe(5–1)	8.8 ± 0.1	2.0 ± 0.1	0.9 ± 0.1	0	0
μHe(>5–1)	4.1 ± 1.6	1.1 ± 0.4	0.4 ± 0.1	0	0

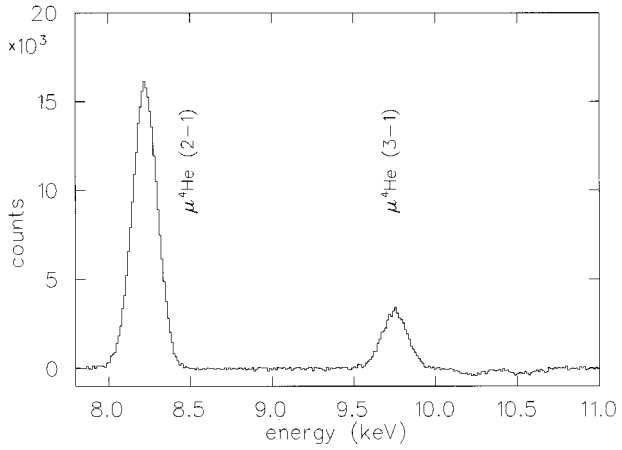

FIG. 9. Spectrum of the Lyman series x rays from μ^4He resulting from excited-state transfer. This spectrum was obtained by subtracting from the total spectrum measured in $H_2+{}^4$He the part due to direct capture in ^{4}He.

ries due to the excited-state transfer are given in Table V. From the total Lyman series intensities in the binary mixtures at our experimental conditions, about $\frac{4}{5}$ are due to transfer from excited states in the $H_2+{}^4$He mixture, and approximately $\frac{3}{4}$ in the $H_2+{}^3$He mixture.

The fraction of muons reaching the ground state in muonic hydrogen after initial $(\mu p)^*$ formation is given by $q_{1s}^{\mathrm{He}}=N_{\mu p}/(N_{\mu p}+N_{\mu p}^*)$. Here $N_{\mu p}$ is the yield of the Lyman series of muonic hydrogen in the binary mixture. $N_{\mu p}^*$ corresponds to the number of μp atoms in an excited state which do not reach the ground state. $N_{\mu p}^*$ is determined from the yield of the Lyman series in muonic helium due to the excited-state transfer. The value of q_{1s}^{He} depends on the density as well as on the concentration. In the $H_2+{}^4$He mixture, we obtained $q_{1s}^{\mathrm{He}}=0.65\pm0.10$, which is in agreement with the theoretical prediction of Ref. [36]. For the $H_2+{}^3$He mixture, the result is $q_{1s}^{\mathrm{He}}=0.50\pm0.10$.

V. CONCLUSION

In our systematic study of the charge exchange of muonic hydrogen to helium [8,16,30,37,38], we investigated the formation and decay of the muonic hydrogen-helium molecules as well as the excited state transfer to the two helium isotopes ^{3}He and ^{4}He.

In binary-gas mixtures $H_2+{}^3$He and $H_2+{}^4$He at about 30 K, the decay of the $(p\mu{}^3\mathrm{He})^*$ and the $(p\mu{}^4\mathrm{He})^*$ molecules was observed with germanium and CCD detectors. The predicted energies, widths, and asymmetrical shapes of the 7-keV transitions are confirmed by our measurements. The total transfer rates $\lambda_{p\mathrm{He}}$ from the muonic hydrogen ground state to ^{3}He and ^{4}He were also obtained from the time distributions of the 7-keV decay x rays. These rates are in agreement with our previous measurements [8], using the triple-gas mixture method. Therefore, average total transfer rates from muonic hydrogen to the two helium isotopes were determined: $\langle\lambda_{p^3\mathrm{He}}\rangle=(0.36\pm0.08)\times10^8\ \mathrm{s}^{-1}$ and $\langle\lambda_{p^4\mathrm{He}}\rangle=(0.49\pm0.05)\times10^8\ \mathrm{s}^{-1}$. The transfer rate to the ^{4}He isotope is in agreement with theoretical predictions [1,14,29]. However, our transfer rate to ^{3}He is lower by a factor of 2–3 than theory. The radiative branching ratios κ for the decay of the muonic hydrogen-helium molecules agree with theory [15,26,32], and confirm the much smaller ratios for the $(p\mu\mathrm{He})^*$ molecules than for the $(d\mu\mathrm{He})^*$ molecules.

In the mixtures $H_2+{}^3$He and $H_2+{}^4$He, the muonic x-ray intensity patterns of the Lyman series in He are significantly different from those in pure He. The difference is due to muon transfer from excited states of muonic hydrogen. This excited-state transfer populates mainly levels with principal quantum numbers $n=2$ and $n=3$. Under our experimental conditions, in the $H_2+{}^4$He measurement, about $\frac{4}{5}$ of the whole μHe Lyman intensities are due to excited-state transfer, and approximately $\frac{3}{4}$ in the $H_2+{}^3$He measurement. The fractions of muons reaching the ground state in muonic hydrogen are $q_{1s}^{\mathrm{He}}=0.65\pm0.10$ in $H_2+{}^4$He and $q_{1s}^{\mathrm{He}}=0.50\pm0.10$ in $H_2+{}^3$He.

ACKNOWLEDGMENTS

We are grateful to O. Huot for his contributions during the experiment, and to K. Danzinger and H. Weiss for their help in the construction of the target cells. The authors are also grateful to E. Kolganova for providing them with theoretical predictions. This work was supported by the Austrian Academy of Sciences, the Austrian Science Foundation, the Beschleunigerlaboratorium der Universität und der Technischen Universität München, the PSI, the Swiss Academy of Science, and the Swiss National Science Foundation.

[1] Y. A. Aristov *et al.*, Yad. Fiz. **33**, 1066 (1981) [Sov. J. Nucl. Phys. **33**, 564 (1981)].
[2] Y. Kino and M. Kamimura, Hyperfine Interact. **82**, 195 (1993).
[3] A. V. Matveenko and L. I. Ponomarev, Zh. Eksp. Teor. Fiz. **63**, 48 (1972) [Sov. Phys. JETP **36**, 24 (1973)].
[4] V. M. Bystritsky *et al.*, Zh. Eksp. Teor. Fiz. **84**, 1257 (1983) [Sov. Phys. JETP **57**, 728 (1983)].
[5] R. Jacot-Guillarmod *et al.*, Phys. Rev. A **38**, 6151 (1988).
[6] R. Jacot-Guillarmod *et al.*, Phys. Rev. A **55**, 3447 (1997).
[7] H. P. von Arb *et al.*, Muon Catal. Fusion **4**, 61 (1989).
[8] S Tresch *et al.*, Phys. Rev. A **57**, 2496 (1998).
[9] J. P. Egger, D. Chatellard, and E. Jeannet, Part. World **3**, 139 (1993).
[10] P. D. Group, Phys. Rev. D **54**, 1 (1996).
[11] V. M. Bystritsky *et al.*, Zh. Eksp. Teor. Fiz. **70**, 1167 (1976) [Sov. Phys. JETP **43**, 606 (1976)].
[12] E. J. Bleser *et al.*, Phys. Rev. **132**, 2679 (1963).
[13] A. V. Kravtsov and A. I. Mikhailov, Phys. Rev. A **49**, 3566 (1994).
[14] A. V. Kravtsov, A. I. Mikhailov, and N. P. Popov, J. Phys. B **19**, 2579 (1986).
[15] A. V. Kravtsov, A. I. Mikhailov, and V. I. Savichev, Hyperfine Interact. **82**, 205 (1993).
[16] B. Gartner *et al.*, Hyperfine Interact. **101/102**, 249 (1996).
[17] B. Lauss *et al.*, Phys. Rev. Lett. **76**, 4693 (1996).

[18] B. Lauss, Ph.D. thesis, University of Vienna, Austria, 1997 (unpublished).
[19] J. P. Egger *et al.*, Muon Catal. Fusion **5/6**, 421 (1990/1991).
[20] *EEV English Electric Valve*, Waterhouse Lane, Chelmsford, Essex, CM1 2QU, England.
[21] D. Chatellard, Ph.D. thesis, University of Neuchâtel, Switzerland, 1995 (unpublished).
[22] B. L. Henke, E. M. Gullikson, and J. C. Davis, At. Data Nucl Data Tables **54**, 181 (1993).
[23] *Mylar Polyester Foil*, Du Pont's registered trademark, Wilmington DE 19898.
[24] *Hostaphan Datenblatt*, Hoechst Diafoil GmbH, Wiesbaden, Germany.
[25] *KAPTON Polyimide Film*, Du Pont's registered trademark, Wilmington DE 19898.
[26] V. Belyaev, O. Kartavtsev, V. Kochkin, and E. A. Kolganova, Z. Phys. D **41**, 239 (1997).
[27] W. Czaplinski, A. Kravtsov, A. Mikhailov, and N. Popov, Phys. Lett. A **233**, 405 (1997).
[28] S. S. Gershtein, Zh. Eksp. Teor. Fiz. **43**, 706 (1962) [Sov. Phys. JETP **16**(2), 501 (1963)].
[29] V. K. Ivanov *et al.*, Zh. Eksp. Teor. Fiz. **91**, 358 (1986) [Sov. Phys. JETP **64**, 210 (1986)].
[30] S. Tresch *et al.*, Euro. Phys. J. D. **2**, 93 (1998).
[31] E. Storm and H. I. Israel, Nucl. Data, Sect. A **7**, 565 (1970).
[32] S. S. Gershtein and V. V. Gusev, Hyperfine Interact. **82**, 185 (1993).
[33] M. Eckhause *et al.*, Phys. Rev. A **33**, 1743 (1986).
[34] G. A. Rinker, Phys. Rev. A **14**, 18 (1976).
[35] F. Kottmann, in *Muonic Atoms and Molecules*, edited by L. A. Schaller and C. Petitjean (Birkhäuser Verlag, Basel, 1993), p. 219.
[36] V. M. Bystritsky, A. Kravtsov, and N. Popov, Zh. Eksp. Teor. Fiz. **97**, 73 (1990) [Sov. Phys. JETP **70**, 40 (1990)].
[37] S. Tresch *et al.*, Hyperfine Interact. **101/102**, 221 (1996).
[38] B. Gartner *et al.*, in *Particles and Nuclei*, edited by C. Carlson and J. Domingo (World Scientific, Singapore, 1997), p. 570.